Cement & Concrete Composites 36 (2013) 109–115

Contents lists available at SciVerse ScienceDirect

Cement & Concrete Composites

journal homepage: www.elsevier.com/locate/cemconcomp

Quartz–titania composites for the photocatalytical modification of construction materials

Sameena Kamaruddin [a], Dietmar Stephan [b,*]

[a] Department of Civil Engineering, University of Kassel, Mönchebergstr. 7, 34125 Kassel, Germany
[b] Department of Civil Engineering, Technische Universität Berlin, Gustav-Meyer-Allee 25, 13355 Berlin, Germany

ARTICLE INFO

Article history:
Received 23 December 2011
Received in revised form 9 August 2012
Accepted 10 August 2012
Available online 21 August 2012

Keywords:
Core–shell-particles
Quartz
Photocatalysis
NO-degradation
Sol–gel-method

ABSTRACT

In this paper the synthesis of photocatalytically modified core–shell composites is reported. The synthesis was realized by hydrolysis and condensation of tetrapropylorthotitanate on ground quartz, which is used as an additive in mortar and concrete. This allowed a controlled growth of titania layers on the particles with different thicknesses. The efficiency of the coating process was studied by interpretation of XRF results. The morphology of the composites was analyzed via SEM. Photoactivity of the particles was studied by analyzing the titania crystal phases of the shell (XRD) and calculating the photonic efficiency of NO-degradation measurements. Moreover methylene blue degradation was performed to reflect the self cleaning properties of the composite materials.

1. Introduction

Since the first photocatalytically modified products were introduced in the East-Asian market, more research works across the world have started focusing on the characteristics, development and application of photocatalysts [1–3]. Titania (TiO_2) has turned out to be the most effective photocatalyst in decomposing organic and inorganic substances and is applied worldwide in different kind of products [4,5]. Especially in the construction engineering sector the application of photocatalysts is very promising. Photocatalytically modified products comprise self-cleaning and air purifying characteristics and are already employed in concrete, glass, mortar etc. for the maintenance of the aesthetic appearance of buildings and the reduction of pollutants [6–8]. Limiting values for pollutants like NO_x, stipulated in the EU Directives on ambient air quality [9,10] are partly exceeded at the moment. For instance, over 50% of the German urban monitoring stations for NO_2 recorded concentrations above the limiting value of 40 $\mu g/m^3$ air in 2010 [11]. In inner-city areas an increase of NO_x emission is furthermore expected and limiting values will be more difficult to achieve. Therefore the application of photocatalytic products for the reduction of NO_x has been tested in laboratories and in pilot projects to assess their potential for air purification [12].

The problem that has been identified with photocatalytic products is a reduced photocatalytic activity in contrast to the pure photocatalyst. Usually the photocatalyst is applied in the form of nanoparticles, to work with a high specific surface area. But this characteristic is also the reason for the high tendency of nanoparticles to agglomerate. As a result, not only nanoparticles exist in the products, but also agglomerates. Therefore a homogeneous and efficient distribution of the photocatalyst is not guaranteed. Hüsken et al. identified agglomerates of TiO_2 formed at the surface of photocatalytically modified paving blocks [13]. Methods to avoid the formation of agglomerates during the mixing process are modifying the concrete mixture by using additives, more water or a high-shear mixer [13]. But mostly the particles are already agglomerated before adding to the concrete mixture and in many cases it is preferred to maintain the mixing formulation. In such cases modified photocatalysts can be the answer.

In this paper the synthesis of such modified photocatalysts, named core–shell composites is reported. By adjusting the size of the systems and applying just a thin layer of titania on a cheaper core material, agglomeration between nano-particles can be avoided and costs can be reduced [14]. Moreover, these systems offer variability in size and thickness of the core and shell respectively. In the last decades silica–titania core–shell composites have been prepared by different methods, such as sol–gel method, flame processes or chemical vapor deposition [15–18]. In many cases synthetically prepared and monodisperse silica cores were used, which represented ideal morphology and purity [19,20]. This work deals with the synthesis of core–shell composites based on

* Corresponding author. Tel.: +30 314 72 100; fax: +30 314 72 110.
E-mail addresses: kamaruddin@uni-kassel.de (S. Kamaruddin), stephan@tu-berlin.de (D. Stephan).

0958-9465/$ - see front matter © 2012 Elsevier Ltd. All rights reserved.
http://dx.doi.org/10.1016/j.cemconcomp.2012.08.007

industrial ground quartz as the core, coated via hydrolysis and condensation of tetrapropylorthotitanate. This provides a base to develop composites, which are applicable for practical purposes. The possibility of changing the shell thicknesses was studied and the photocatalytical activities were determined.

2. Materials and methods

2.1. Preparation of the functional composites

Industrial quartz powder, Millisil W12 (Quarzwerke Frechen, Germany) with an upper grain size of d_{95} = 50 μm was used as the core material and tetrapropylorthotitanate (TPOT) (Merck, Germany) for obtaining the titania shell.

For the coating process the quartz particles were dispersed ultrasonically in an ethanol/water mixture with a water content of 1 mol/L. The resulting silica dispersion was 14 wt.%. Different amounts of an ethanolic TPOT solution with 28 wt.% were added with a feed rate of 0.5 ml/min to the silica sol under continuous stirring at room temperature (20 °C). The amounts of added TPOT were equal to different weight percentages of titania in case of complete hydrolyzation. The dosages were calculated on the basis of the molecular weights of SiO_2 and TiO_2. Data are given in Table 1.

The preparation was stirred for about 20 h following centrifugation and washing steps with ethanol until the supernatant was clear. Afterwards the coated particles were dried and calcined at 650 °C. Finally the samples were centrifuged and washed again, to remove possible titania-shell splinters.

2.2. Characterization

2.2.1. Physico-chemical characterization

Quantitative X-ray fluorescence analysis (XRF) was performed (*according to DIN/EN/ISO 12677)* by using an X-ray fluorescence spectrometer (PANalytical Axios, Netherlands) [21]. The particle size analysis of coated and uncoated particles was performed via a Laser Granulometer (Beckman Coulter, LS 230, USA). Data of specific surface area were collected through the BET physisorption method (Autosorb-1 Quantachrome, USA) [22]. Morphology of the particles was examined using a scanning electron microscope (SEM, Carl Zeiss Supra 40VP, Germany) with voltages between 3 and 15 kV and a secondary electron detector. All specimens were sputter-coated with gold prior to SEM-analysis. X-ray diffraction (XRD) analysis was carried out with a D4 X-ray diffractometer (Bruker AXS, Germany) at a voltage of 30 kV, a current of 40 mA and a Lynx-Eye detector.

Table 1
Amounts of quartz and ethanolic TPOT solution for the preparation.

Sample (wt.% SiO_2/wt.% TiO_2)	Millisil W12 (g)	TPOT solution (g)
90/10	50	70.6
80/20	50	158.8
70/30	50	272.2
60/40	50	423.5

2.2.2. Photocatalytical characterization

Photocatalytic activity was tested via two different methods.

Degradation of methylene blue (MB) was examined in an aqueous solution with an apparatus designed after DIN 52980 [23]. 30 mg of each sample was sedimented in 40 ml of an aqueous 10 μmol/L MB-solution, in a cylindrical glass beaker (∅ = 3 cm). The solutions were kept in the dark for two hours after which the samples were irradiated with UV-A light having an intensity of about 1.7 mW/cm^2 for another 18 h. Illumination was provided by two 20 W UV-lamps (Philips Cleo).

NO-degradation was studied via an apparatus designed after ISO 22197-1 [24]. The sample container made of acrylic glass with a cover made of quartz, had an area of 25 cm^2 and a volume of 2.5 cm^3 and was completely filled with the sample to be tested. NO gas with a concentration of 1 ppm was streamed over this testing area. Prior to the measurements, the samples were pre-exposed to UV-A light of 1 mW/cm^2 intensity for seven days. This ensured that pollutants, which were already on the sample, were degraded.

The two test setups are illustrated in Fig. 1.

3. Results and discussion

3.1. XRF chemical analysis

TPOT is an organic titania precursor and reacts to TiO_2 via hydrolysis and condensation as the chemical equation (1) describes

$$[Ti(OC_3H_7)_4] + 2H_2O \rightarrow TiO_2 + 4C_3H_7OH \quad (1)$$

When quartz particles were added to the reaction, titania monomers adsorbed on the quartz surface. Chemisorption and physisorption were both possible. In case of chemisorption titania

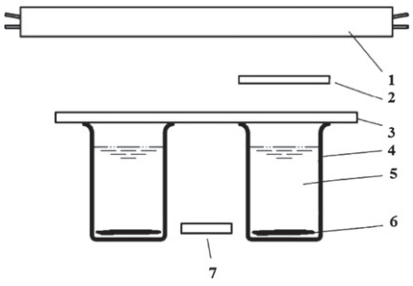

1 light source
2 cover against UV-light
3 glass cover
4 testing chamber
5 methylene blue solution
6 tested sample
7 photometer

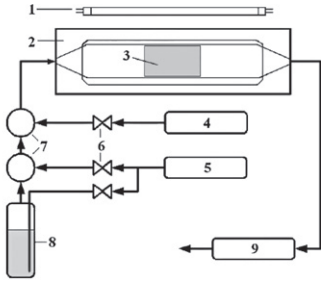

1 light source;
2 optical window;
3 testing area (25cm^2)
4 gas containing the pollutant;
5 purified air;
6 mass-flow controllers;
7 gas mixers;
8 humidifier;
9 analyzer for pollutants

Fig. 1. Schematic drawing of the setup for analysis of MB-degradation after DIN 52980 (left) and NO-degradation based on ISO 22197-1 (right) [24].

was chemically bound on the surface, in case of physisorption small titania aggregates physically adsorbed on the surface via van der Waals forces. In such a case, it was possible that very weakly bonded aggregates were removed during the washing step.

XRF measurements were performed to study the efficiency of the coating procedure. The XRF analysis yielded the real quantities of silica and titania in the samples after washing and calcination at 650 °C and therefore gave information about the efficiency of the hydrolysis and the loss of particles during the preparation process. The sample names in this study equate to the percentage weight ratios of quartz and titania, in case of complete transformation of the TPOT precursor to titania on the quartz surface. For example 60/40 equates to 60 wt.% SiO_2 and 40 wt.% TiO_2.

These theoretically calculated values were compared to the data of the XRF analysis in Table 2. The results show that the sample compositions of the two samples with lower concentration of TiO_2 are very close to the theoretically defined ones. The samples with 30 and 40 wt.% of TiO_2 do not follow the trend and it seems that approx. 20 wt.% TiO_2 is the maximum which can be bound to the given surface of the quartz powder.

3.2. BET specific surface area

The BET specific surface area of uncoated particles washed and calcined at 650 °C was 0.69 m^2/g, which is in good agreement with the value of 0.9 m^2/g given by the manufacturer.

Data of the BET surface analysis showed that the specific surface area increased after coating with titania (see Fig. 2). The adsorption of smaller titania aggregates caused a rougher surface, which increased the specific surface area. The smaller the aggregates are, the higher the specific surface is. The maximum specific surface area was achieved for samples 80/20. The reason for the similar BET values of sample 80/20, 70/30 and 60/40 can be due to the similar titania quantities in these three samples. The results correlate very well with the XRF results.

3.3. SEM analysis

By using a scanning electron microscope the morphology of uncoated and coated quartz particles could be studied. Uneven surfaces for uncoated particles were observed, as can be seen in Fig. 3 in different magnifications. Tiny quartz splinters spread on the surface as well as calderas and small holes could be identified, too.

Fig. 4 illustrates several coated quartz particles of sample 70/30 before calcination. This shows that the quartz particles were successfully covered by titania. Moreover the micrographs reveal that the titania cover is not continuous, as it contains many cracks. More and deeper cracks were observed for thicker coatings. The

Table 2
Quantities of titania and silica analyzed via XRF.

Sample	(SiO_2 wt.%/TiO_2 wt.%)	90/10	80/20	70/30	60/40
XRF	SiO_2 [wt.%]	91	81	74	81
XRF	TiO_2 [wt.%]	8	18	25	18

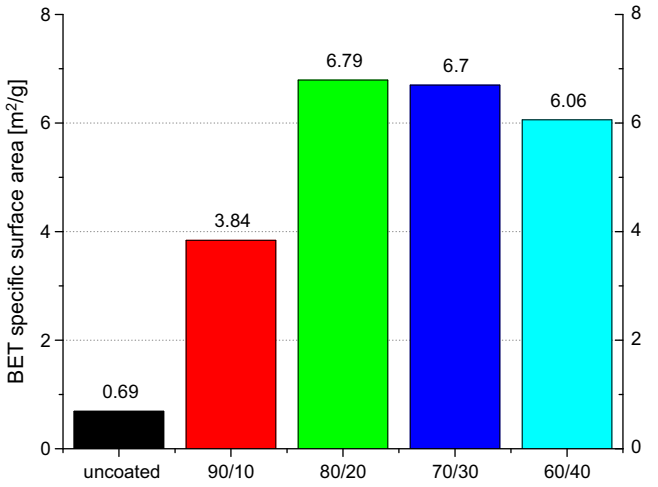

Fig. 2. BET specific surface area determined via gas adsorption analysis of uncoated and coated samples after calcination at 650 °C.

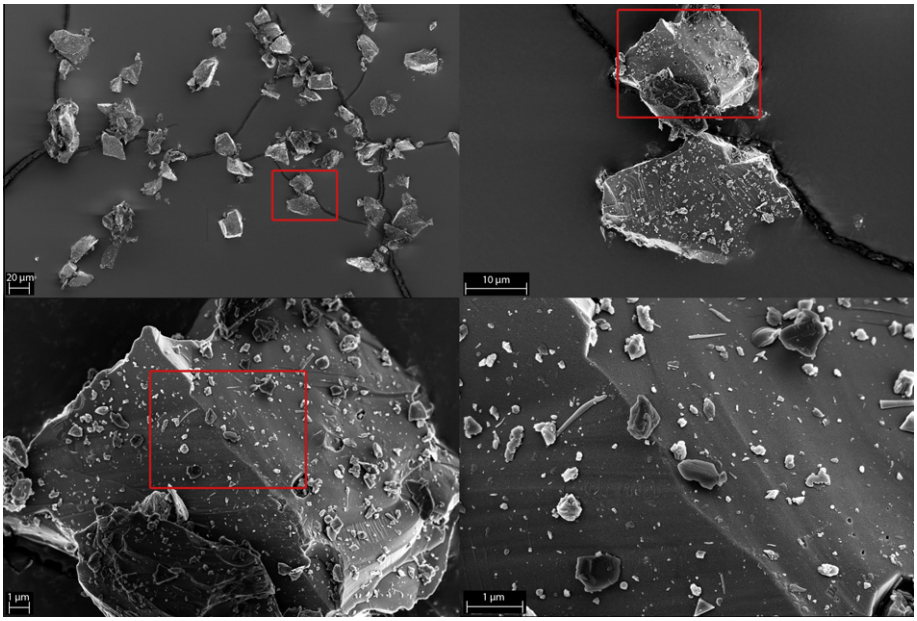

Fig. 3. Micrographs of uncoated quartz particles in different magnifications.

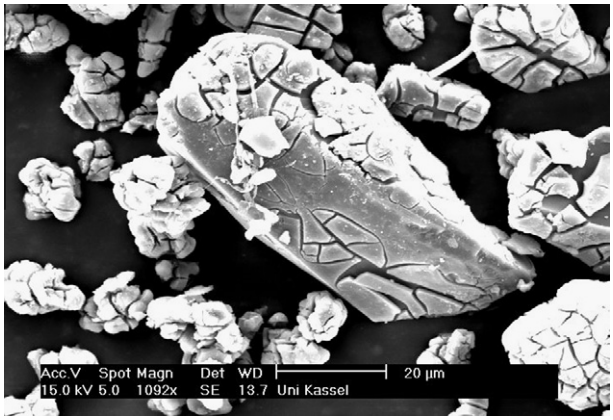

Fig. 4. Sample "70/30" after drying at 40 °C.

reason for this is the high water content of the initial titania coating and the thermal stress resulting out of it during the drying-process. This postulation was supported by the observation of more distinctive cracks in case of the calcined particles that have undergone a higher thermal stress (see Fig. 5).

Fig. 5 shows several micrographs of a coated and calcined particle taken at different magnifications. This also allows a closer look at the titania layer, where it is clearly visible that the layer is made up of aggregated titania monomers of nanoscaled dimensions.

A collection of all coated samples together with close ups of their shells is presented in Fig. 6.

As the quartz particles did not consist of even surfaces, the coating thickness also varied from one area to another area on one particle and also between the particles within one sample. It has to be considered, that each core particle was shaped differently. The shape has an influence on the adsorption of the titania monomers. On some particles a thicker layer might have been developed, whereas other particles possess thinner coatings or uncoated areas, especially those particles with more sharp edges and lines. However, the shell thicknesses increased with higher amounts of titania in the samples and the trend correlates well with the XRF data.

3.4. XRD analysis

XRD analysis was performed to study the mineralogical phase composition of the samples. Only the anatase phase was found in the coated samples as the XRD pattern reveals (Fig. 7). Moreover it was discovered that sample 80/20 showed the highest crystallinity, as the sharpest peaks were found in that pattern.

3.5. Photocatalytical characterization

Methylene blue (MB) degradation after DIN 52980 was performed to reflect the self cleaning properties of the composite materials. The degradation of NO gas after ISO 22197-1 [24] represents their capability to degrade air pollutants and remarks their potential for the development of construction materials with environmentally beneficial character. Technical data and operation details as well as schemes of the test setups are given in Section 2.2.2. The results of both methods are shown in Figs. 8 and 9.

MB-degradation was tested for all samples and also for three different calcination temperatures, exemplarily for sample 70/30 (Fig. 8). The results revealed the temperature of 650 °C as the most effective calcination temperature. A comparative study of all samples identified sample 80/20 to be the most active one. One reason for this could be the high crystallinity of that sample as found via XRD. In highly crystalline materials fewer defects are observed. For the photocatalytical degradation reaction radicals play an important role, which are formed by electrons and holes generated in the titania particle. Crystal defects promote the recombination of electrons and holes and fewer radicals can be formed. But even sample 90/10 showed higher activities than sample 70/30 and 60/40 which contained higher amounts of titania. As the amount of titania was very low, peaks in the XRD pattern were not observed for sample 90/10, which does not mean that the sample did not consist of highly crystalline anatase. Photocatalytic activity does also depend on the amount of titania exposed to the UV-light.

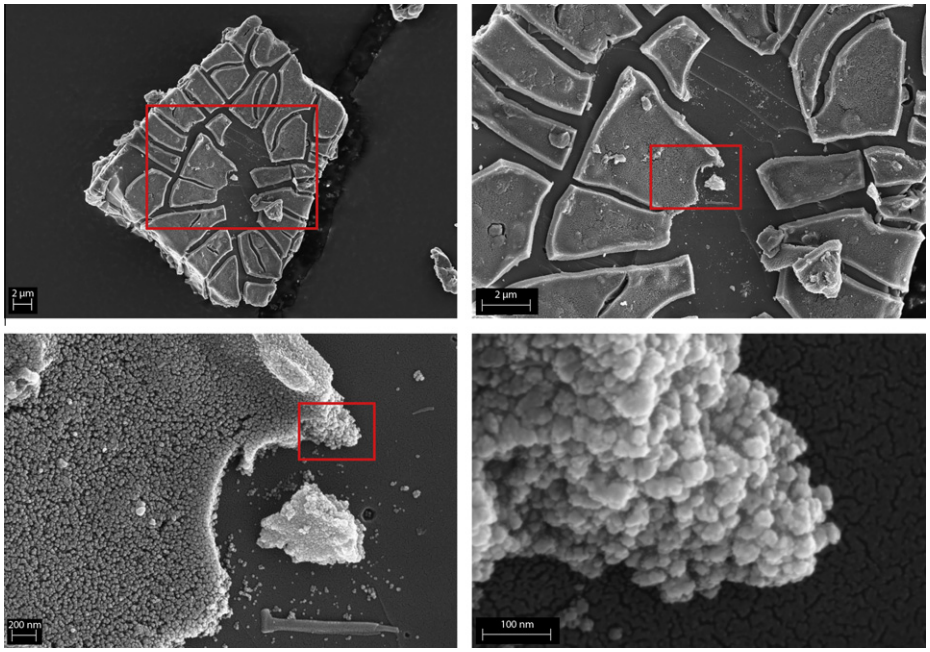

Fig. 5. Micrographs taken at different magnifications of sample "80/20" after calcination at 650 °C.

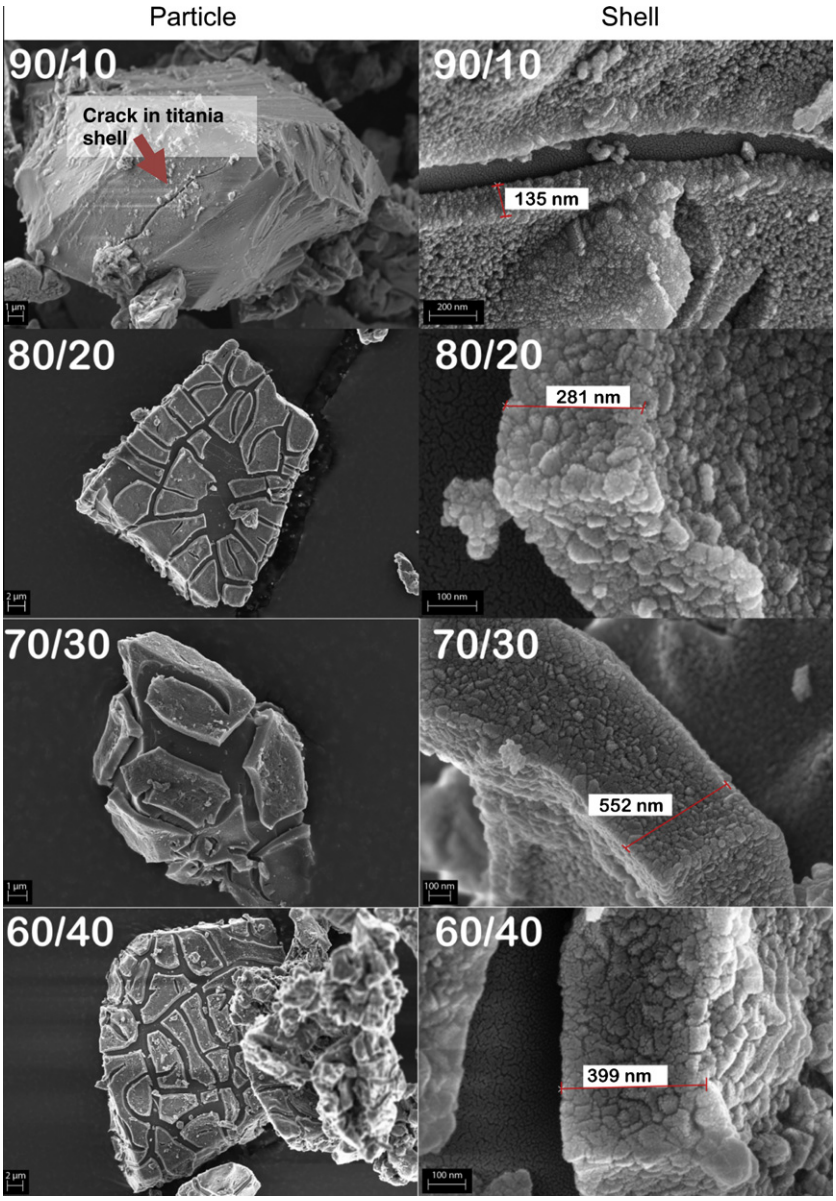

Fig. 6. Micrographs of all coated samples calcined at 650 °C and shell thicknesses.

Some samples consisted of more cracks or thinner titania layers. In both cases a higher amount of the total titania in the sample is exposed to the UV-light and can therefore be activated for the degradation reactions.

When looking at the results of the NO-degradation test, increasing photonic efficiencies were found with higher amounts of TPOT added (Fig. 9). The photonic efficiency is defined here as the ratio of the NO-degradation rate and the incident photon flux, for a mean irradiation wavelength of 350 nm. The photonic efficiency ζ was calculated via the following equations [25]:

$$I_0 = \frac{I\lambda}{N_A hc} \quad I_0 = \text{light flux}$$

I = light intensity (J s^{-1} cm^{-2})

N_A = Avogadro constant (mol^{-1})

h = Planck's constant (J s) c = light velocity (m s^{-1})

λ = wavelength (m) (2)

$$\zeta(\%) = \frac{\Delta n_{NO}}{I_0 \cdot A} \times 100$$

Δn_{NO} = difference in inlet and outlet fluxes of NO (mol s^{-1})

A = illuminated area (cm^2).

Samples 60/40 and 70/30 showed the highest photonic efficiencies. Moreover the results revealed that standard nanoscaled photocatalysts (P25 and Hombikat UV 100) measured under the same conditions showed lower efficiencies than these two samples. The reason for the high photoactivities can be the high surface areas of these two samples. Sample 60/40 consisted of a lower XRF identified amount of titania than sample 70/30 and almost of the same amount as sample 80/20. Still photonic efficiency was highest for this sample. It can be suspected that the high surface area, the amount of NO molecules adsorbed on the sample surface and the amount of titania exposed to the UV-light, which varied due to cracks in the shell, were the influencing factors. The photocatalytic activity also depends on the

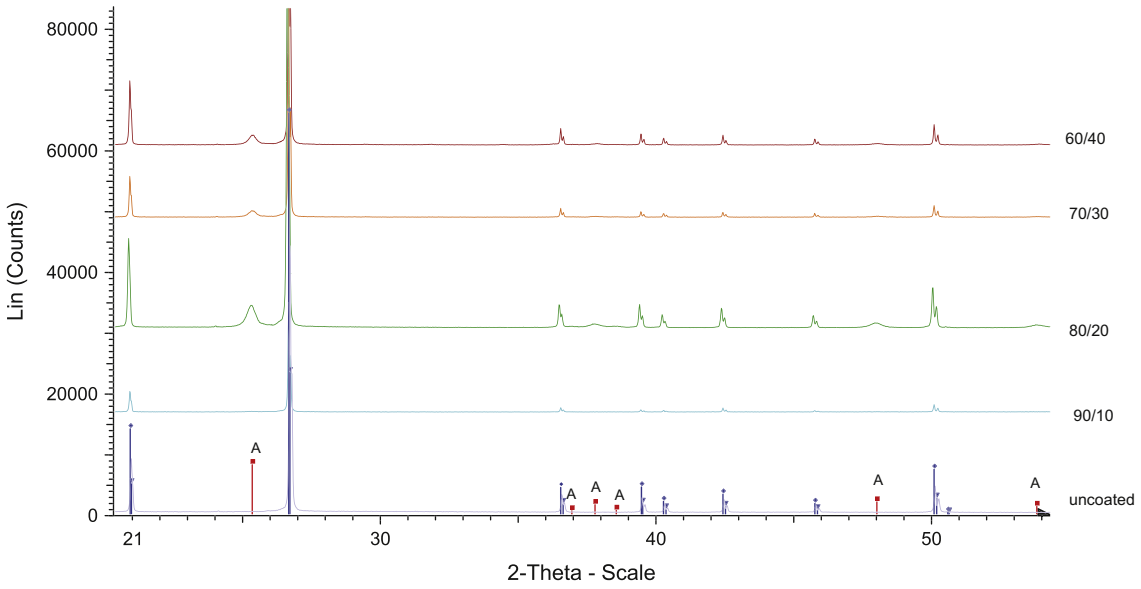

Fig. 7. XRD patterns of coated and uncoated samples after calcination at 650 °C. (Anatase peaks are marked with an A, the other peaks are those of the quartz core.)

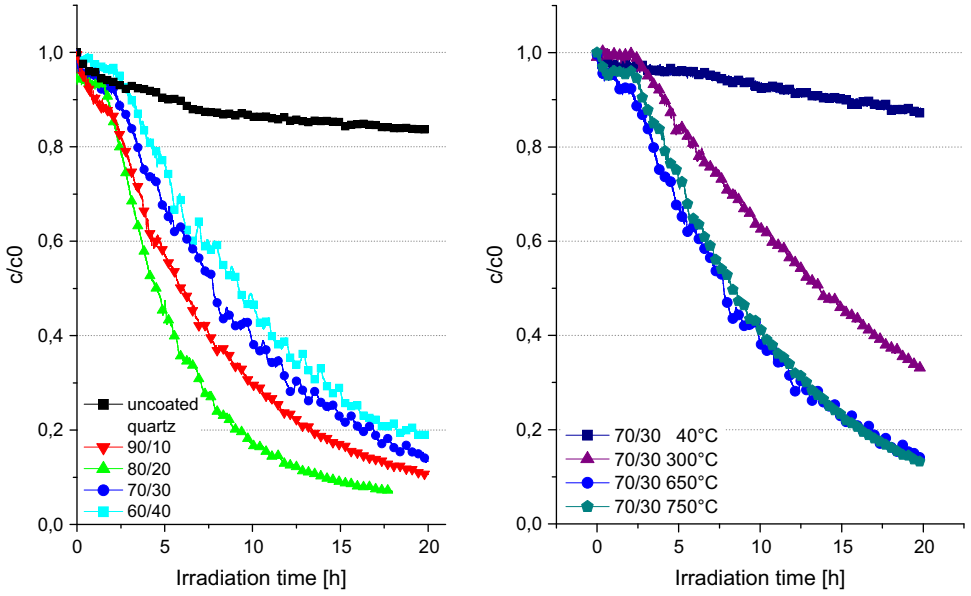

Fig. 8. Relative MB-concentration (c/c_0) by irradiation time of all samples calcined at 650 °C (left) and sample "70/30" calcined at different temperatures (right).

amount of surface hydroxyl groups and surface bound water that reacts to radicals with electrons and holes respectively. The exact reason is not clear.

The results of MB- and the NO-degradation test cannot directly be compared with each other and therefore have to be examined independently. In case of NO-degradation there was a lower humidity in the gas reaction chamber. In contrast the MB-test was performed in an aqueous solution of MB. Light intensity was also lower and the testing areas were different.

4. Conclusions

Quartz–titania composites were successfully derived by hydrolysis and condensation of TPOT using ground quartz (d_{95} = 50 μm) as the core material. The results indicated that 20 wt.% TiO_2 was the maximum which could be bound to the given surface of the quartz powder. The formation of shell thicknesses between approximately 100–550 nm of the sol–gel derived titania layers could be controlled by supplying different amounts of TPOT during the coating process. After calcination at 650 °C the shells were composed of only the anatase phase. The shells were not continuous and consisted of cracks, which are advantageous for the photocatalytic activity, as more active surface area of titania was bared. All samples showed successful decomposition of MB and NO. Two samples showed photonic efficiencies, which were above those of P25 and Hombikat UV 100, frequently used as benchmarks for photocatalysts. The results make the composites appealing for application in building materials as the problem of agglomeration between nanoparticles can be avoided. Therefore an efficient distribution of the photocatalyst in mortar mixtures for instance is expected. Further studies are going on to test these postulations.

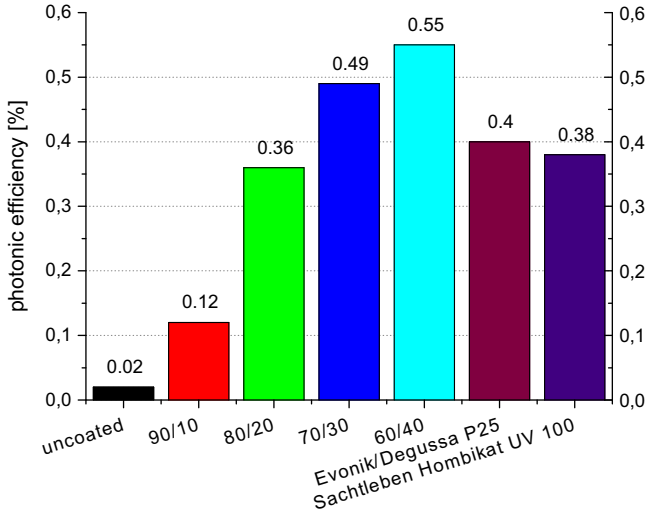

Fig. 9. Photonic efficiencies of the NO-degradation test for uncoated quartz and all coated samples.

Acknowledgments

The work is part of the project "HelioClean". The authors would like to acknowledge the financial support from the German Federal Ministry of Education and Research (BMBF). The SEM micrographs were taken at the University of Dresden with Markus Günther, whom we would also like to thank for his support.

References

[1] Kaneko M, Okura I. Photocatalysis: science and technology. Berlin: Springer; 2002.
[2] Xia XH, Liang Y, Wang Z, Fana J, Luo YS, Jia ZJ. Synthesis and photocatalytic properties of TiO_2 nanostructures. Mater Res Bull 2006:2187–95.
[3] Wilhelm P, Stephan D. Titandioxid für selbstreinigende Beschichtungen von Baustoffen. Beton 2007(5):202–5.
[4] Liu I, Lawton LA, Bahnemann DW, Robertson PKJ. The photocatalytic destruction of the cyanotoxin, nodularin using TiO_2. Appl Catal B 2005;60(3–4):245–52.
[5] Muneer M, Saquib M, Qamar M, Bahnemann D. Titanium-dioxide-mediated photocatalysis reaction of three selected pesticide derivatives. Res Chem Intermediat 2004;30(6):663–72.
[6] Hunger M, Hüsken G, Brouwers J. Photocatalysis applied to concrete products – part 1: principles and test procedure. ZKG Int 2008;61(8):77–85.
[7] Hüsken G. Concrete containing TiO_2: properties and evaluation of air purifying abilities. In: Fib-symposium; 2008. p. 26–5.
[8] Amadelli R, Cassar L, Pepe C. Use of photocatalytic preparations of colloidal titanium dioxide for preserving the original appearance of cementitious, stone or marble products: PCT; B05D 1/36(US 6,824,826 B1); 2004.
[9] The Council of the European Union. Council directive 96/62/EC on ambient air quality assessment and management; 1996.
[10] The European Parliament and the Council of the European Union. Directive 2008/50/EC of the European Parliament and the Council on ambient air quality and cleaner air for Europe; 2008.
[11] Umweltbundesamt. Luftbelastungssituation 2010; 2011.
[12] Picada EC GRD1-2001-40449. Innovative facade coatings with de-soiling and de-polluting properties:31 official presentation: European Commission; 2006.
[13] Hüsken G, Hunger M, Brouwers H. Photokatalytische Betonprodukte. BFT 2009;12:28–33.
[14] Kamaruddin S, Stephan D. The preparation of silica–titania core–shell particles and their impact as an alternative material to pure nano-titania photocatalysts. Catal Today 2011;161(1):53–8.
[15] Fu X, Qutubuddin S. Synthesis of titania-coated silica nanoparticles using non-ionic water-in-oil. Colloid Surf A 2001;178(1–3):151–6.
[16] Hu Y, Li C, Gu F, Zhao Y. Facile flame synthesis and photoluminescent properties of core/shell TiO_2/SiO_2 nanoparticles. J Alloy Compd 2007;432(1–2):L5–9.
[17] Wilhelm P, Stephan D. On-line tracking of the coating of nanoscaled silica with titania nanoparticles via zeta-potential measurements. J Colloid Interface Sci 2006;293(1):88–92.
[18] Kalele S, Gosavi SW, Urban J, Kulkarni SK. Nanoshell particles: synthesis, properties and applications. Curr Sci India 2006;91(8):1038–52.
[19] Kim KD, Bae HJ, Kim HT. Synthesis and characterization of titania-coated silica fine particles by semi-batch process. Colloid Surf A 2003;224(1–3):119–26.
[20] Lim SH, Phonthammachai N, Pramana SS, White TJ. Simple route to monodispersed silica–titania core–shell photocatalysts. Langmuir 2008;24(12):6226–31.
[21] DIN EN ISO 12677:2012–01. Chemische analyse von feuerfesten Erzeugnissen durch Röntgenfluoreszenz-analyse (RFA) – Schmelzaufschluss-Verfahren (ISO 12677:2011). Deutsche Fassung EN ISO 12677; 2011.
[22] Brunauer S, Emmet PH, Teller T. Adsorption of gases in multimolecular layers. Org Synth 1938;1:309–19.
[23] DIN 52980. Photokatalytische Aktivität von Oberflächen – Bestimmung der photokatalytischen Aktivität im wässrigen Medium durch Abbau von Methylenblau. DIN 52980; 2008.
[24] International Standard ISO 22197-1. Fine ceramics (advanced ceramics, advanced technical ceramics) – test method for air-purification performance of semiconducting photocatalytic materials. Part 1 – Removal of nitric oxide; 2007.
[25] Kandiel TA, Dillert R, Feldhoff A, Bahnemann DW. Direct synthesis of photocatalytically active rutile TiO_2 nanorods partly decorated with anatase nanoparticles. J Phys Chem C 2010;114(11):4909–15.